Received: 19 November 2018 | Accepted: 13 September 2019

DOI: 10.1002/hyp.13603

RESEARCH ARTICLE

WILEY

The compensating effect of glaciers: Characterizing the relation between interannual streamflow variability and glacier cover

Marit van Tiel[1] | Irene Kohn[1] | Anne F. Van Loon[2] | Kerstin Stahl[1]

[1]Environmental Hydrological Systems, Faculty of Environment and Natural Resources, University of Freiburg, Freiburg, Germany

[2]School of Geography, Earth and Environmental Sciences, University of Birmingham, Birmingham, UK

Correspondence
Marit van Tiel, Environmental Hydrological Systems, Faculty of Environment and Natural Resources, University of Freiburg, Freiburg, Germany.
Email: marit.van.tiel@hydrology.uni-freiburg.de

Funding information
Deutsche Forschungsgemeinschaft, Grant/Award Numbers: DFG STA632/4-1, STA632/3-1

Abstract

Meltwater from glaciers is not only a stable source of water but also affects downstream streamflow dynamics. One of these dynamics is the interannual variability of streamflow. Glaciers can moderate streamflow variability because the runoff in the glacierized part, driven by temperature, correlates negatively with the runoff in the non-glacierized part of a catchment, driven by precipitation, thereby counterbalancing each other. This is also called the glacier compensation effect (GCE), and the effect is assumed to depend on relative glacier cover. Previous studies found a convex relationship between streamflow variability and glacier cover of different glacierized catchments, with lowest streamflow variability at a certain optimum glacier cover. In this study, we aim to revisit these previously found curves to find out if a universal relationship between interannual streamflow variability and glacier cover exists, which could potentially be used in a space-for-time substitution analysis. Moreover, we test the hypothesis that the dominant climate drivers (here precipitation and temperature) switch around the suggested optimum of the curve. First, a set of virtual nested catchments, with the same absolute glacier area but varying non-glacierized area, were modelled to isolate the effect of glacier cover on streamflow variability. The modelled relationship was then compared with a multicatchment data set of gauged glacierized catchments in the European Alps. In the third step, changes of the GCE curve over time were analysed. Model results showed a convex relationship and the optimum in the simulated curve aligned with a switch in the dominant climate driver. However, the multicatchment data and the time change analyses did not suggest the existence of a universal convex relationship. Overall, we conclude that GCE is complex due to entangled controls and changes over time in glacierized catchments. Therefore, care should be taken to use a GCE curve for estimating and/or predicting interannual streamflow variability in glacierized catchments.

KEYWORDS

glacier compensation effect, glacierized catchments, interannual variability, modelling experiment, space-for-time substitution, streamflow

1 | INTRODUCTION

Streamflow variability is related to climate variability, for instance heat waves, seasonality of precipitation and temperature, and climate modes (e.g., Barlow, Nigam, & Berbery, 2001; Dettinger & Diaz, 2000), and moderated by catchment storages, such as lakes, groundwater and soil characteristics (e.g., Andrés Doménech, García Bartual, Montanari, Segura, & Bautista, 2015; Milly & Wetherald, 2002). In mountain regions, snow and particularly glaciers represent such storages that can modify the streamflow response to climate input (e.g., Collins, 2006a; Dahlke, Lyon, Stedinger, Rosqvist, & Jansson, 2012; Fleming & Dahlke, 2014; Jansson, Hock, & Schneider, 2003; Jenicek, Seibert, Zappa, Staudinger, & Jonas, 2016, Viviroli et al., 2011). Many timescales of variability exist, for example daily variations, intra-annual and interannual variability, and decadal variability. In mountain regions, interannual variability of streamflow is particularly important because it characterizes the reliability of water supply for diverse water uses, for example, hydropower (Schaefli, Manso, Fischer, Huss, & Farinotti, 2019). The interannual streamflow variability of glacierized catchments will therefore be the focus of this study.

In mountain regions, glaciers can decrease the streamflow variability in partly glacierized catchments because the glacierized part of the catchment has an opposite runoff regime compared with the non-glacierized part of the catchment, thereby counterbalancing each other (Braithwaite & Olesen, 1988; Meier & Tangborn, 1961; Rothlisberger & Lang, 1987). The non-glacierized part is characterized by a rainfall-runoff regime and the glacierized part by a melt-dominated regime. This means that, in a catchment where both of these runoff regimes are present, during warm and dry periods, the melt from the glacierized part could compensate for the lack of precipitation in the non-glacierized part (e.g., Koboltschnig, Schöner, Holzmann, & Zappa, 2009; Zappa & Kan, 2007). On the other hand, during cold and wet periods, runoff from the non-glacierized part could compensate for the lack of melt from the glacierized part (e.g., Hopkinson & Young, 1998). This process is called the glacier compensation effect (GCE, e.g., Fountain & Tangborn, 1985; Rothlisberger & Lang, 1987).

How much the two different hydrological regimes in a glacierized catchment can counterbalance each other is considered to depend on the relative area of the glacierized part and the non-glacierized part (e.g., Fountain & Tangborn, 1985), that is, the catchment's glacier cover fraction (g). If the non-glacierized part covers a large part of the catchment, precipitation variability will mainly control streamflow variability. If on the other hand the glacier covers a large part of the catchment, streamflow variability is dominated by temperature variability (e.g., Casassa, López, Pouyaud, & Escobar, 2009; Collins, 2006a; Rothlisberger & Lang, 1987). Several empirical studies looked at the relation between g and streamflow variability, expressed as the coefficient of variation (CV_Q) for different samples of catchments (Braithwaite & Olesen, 1988; Chen & Ohmura, 1990; Collins, 2006b; Fleming & Clarke, 2005; Fountain & Tangborn, 1985; Krimmel & Tangborn, 1974; Meier & Tangborn, 1961; Moore, 1992), and some of them found a convex nonlinear relationship with higher CV_Q at low and high g (Chen & Ohmura, 1990; Fountain & Tangborn, 1985). This convex relationship (see conceptual curve in Figure 1) was found to have an optimum (minimum CV_Q, maximum compensation, GCE_{opt}) at 36% g for a U.S. data set (Fountain & Tangborn, 1985) and at 39–44% g for a data set in the European Alps (Chen & Ohmura, 1990). Most of the other studies only looked at a small sample of glacierized catchments and were therefore only able to confirm parts of the relationship. Moreover, Moore (1992) and Collins (2006b) discuss that finding a relation between g and CV_Q can be complicated because other factors than just g, for example, elevation range, glacier hypsometry, climate characteristics, and snow on the glacier, influence the interplay between runoff from the glacierized part (Q_{gl}) and the non-glacierized part (Q_{nongl}).

Despite these few empirical studies that suggest a nonlinear convex relationship between g and CV_Q, later research has not built on these studies to establish a universal relationship for the influence of glaciers on streamflow variability. However, some studies used the relationships found to estimate and/or compare CV_Q (e.g., Hopkinson & Young, 1998). Also, research into the processes' relative importance underlying the hypothesized curve has been limited. This is in stark contrast to the many studies that mention the compensation effect of glaciers as general motivation for why it is important to study the role of glaciers in hydrology. If a universal relationship could be found, it would help to better understand spatial differences in flow reliability. This would have a number of advantages for water resources planning such as decisions on where to install small hydropower plants or intakes for water supply (Gaudard et al., 2014; Schaefli et al., 2019).

Also, if a universal relationship between g and CV_Q existed, it could be used to estimate how CV_Q of a specific catchment would change over time due to deglaciation (following the GCE curve from right to left), which is crucial information for water management and planning. The intraregional comparison of catchments' CV_Q and g in previous studies might thus be interpreted as a space-for-time substitution (Singh, Wagener, Werkhoven, Mann, & Crane, 2011). This

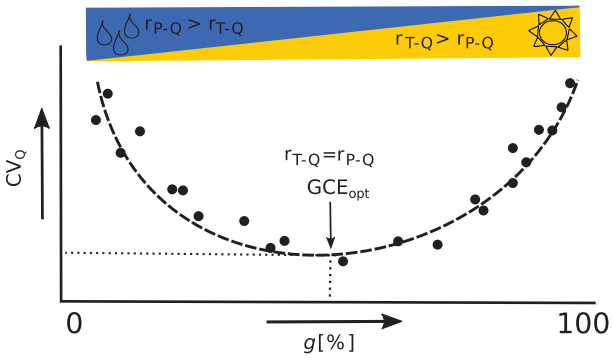

FIGURE 1 Conceptual understanding of GCE curve, after Chen and Ohmura (1990). CV_Q is the coefficient of variation and represents interannual streamflow variability, g is the relative glacier cover, and GCE_{opt} indicates the optimum g where CV_Q is lowest. $r_{P\text{-}Q}$ and $r_{T\text{-}Q}$ are the correlations of streamflow with precipitation and temperature, respectively

translation, going from a relationship based on different catchments to a relationship for one catchment over time, has recently been applied for the Budyko curve (Carmona, Sivapalan, Yaeger, & Poveda, 2014; Sivapalan, Yaeger, Harman, Xu, & Troch, 2011). Hock, Jansson, and Braun (2005) already interpreted the GCE curve as a space-for-time substitution. They hypothesized that under global warming, the interannual variability of streamflow will first decrease (or, depending on initial g, increase) and increase later on. However, we argue that before any time interpretations of the curve are made, a more systematic analysis of the compensation effect and the relationship between g and CV_Q is needed.

The GCE curve, as sketched in Figure 1, could be interpreted in three ways:

1 several nested catchments with the same absolute glacier area but different g due to larger/smaller non-glacierized area (with outlet further downstream/upstream);
2 different catchments within a specific region (e.g., Chen & Ohmura, 1990); and
3 one catchment with changing g over time due to deglaciation (e.g., hypothesized by Hock et al., 2005).

A data set of the first type has not been used to define or corroborate a GCE curve yet, most likely because there is no appropriate streamflow data set available from several nested undisturbed catchments with the same absolute glacier area covering a g range large enough to fit or test a relationship. Neither has an examination of the climate drivers of streamflow variability in relation to the GCE curve been carried out. We hypothesize that precipitation is the dominant driver of streamflow variability below GCE_{opt}, and temperature is the dominant driver above GCE_{opt}. So, catchments to the right of the optimum would have a higher correlation of streamflow with temperature ($r_{T\text{-}Q}$) than with precipitation ($r_{P\text{-}Q}$) and vice versa for catchments to the left of the optimum (Figure 1). If data can confirm this hypothesis, then the correlation of streamflow with temperature and precipitation might be an indicator of the catchments' location relative to the optimum.

In this study, we test the different interpretations of the GCE curve and its climate controls with the aim of challenging the existence of a universal (convex) relationship between streamflow variability and glacier cover. This will give a better insight in whether the relationship can be used for planning and predictions of future water reliability in glacierized catchments under climate change. By a universal relationship we mean that, for a certain region, a convex relationship can be fitted through some data points and that other catchments, as well as a particular catchment during deglaciation, in this region follow(s) this curve.

The study is organized as follows: First, we perform a model experiment with virtual nested catchments (Interpretation 1 as mentioned above) to isolate the effect of g on CV_Q, to look at the streamflow components Q_{gl} and Q_{nongl}, and to investigate the climate drivers. Next, the modelled relationship is compared with observation data of catchments in the Swiss and Austrian Alps (Interpretation 2) to examine whether such a GCE relationship can be found for the region of the Alps and to confirm or reject, with more recent data, the previously found relationship for the Alps (from Chen & Ohmura, 1990). In addition to the g–CV_Q relationship, correlations with climate drivers are analysed. Last, we explore the time aspect of the relationship (Interpretation 3). We evaluate the g–CV_Q relationship in different periods and analyse changes of CV_Q over time for a selection of long streamflow records.

2 | DATA AND METHODS

2.1 | Model experiment

As a first step in analysing the relationship between CV_Q and g, a model experiment was carried out (e.g., Rees & Collins, 2006). A virtual nested catchment model framework enabled the analysis of the compensating effect in a controlled way. Nested catchments form a natural laboratory to analyse the influence of differences in g while most other factors are similar. Specifically, we aim to test if realizing this nested catchment approach by hydrological modelling results in a convex relationship as hypothesized.

The setup of our virtual nested model catchments is based on a real catchment, using observed glacier geometries and area elevation distributions (Figure 2). The catchment taken as starting point is the Schwarze Lütschine, located on the north side of the Swiss Alps. The glacier outline for the year 1973 and a digital elevation model were used to define the glacierized area and elevation zones with a 100-m interval. g in the original catchment, comprising subcatchments 1–4, is 20.1% (36.1 km^2). To design model catchments with $0\% < g < 100\%$, we decreased (increased) the non-glacierized area of the original catchment to increase (decrease) g. In this way, we vary g, but keep glacier geometry constant and climate input comparable between the different nested model catchments.

Increasing g was done by removing the subcatchments (Table 1, Figure 2), one after the other, thereby reducing the original catchment area. Adding additional non-glacierized area to the original catchment required a virtual approach because the outlet in the real setting cannot be moved further downstream (another glacierized tributary joining and the river ending in Lake Brienz). Therefore, a clone of subcatchment 1 was added as many times as was needed to create a model catchment with g of 15%, 10%, 5%, 3%, and 1% (Table 1). For the lowest g (0%) model catchment, we took the virtual catchment g_1 (Table 1), and changed the glacier area in this catchment into non-glacierized area. For g_{100}, the catchment area corresponded to the glacier area.

The HBV-light software (Seibert & Vis, 2012; Seibert, Vis, Kohn, Weiler, & Stahl, 2018) was used to model the streamflow of these nested glacierized catchments. HBV-light is a semidistributed model based on hydrological response units defined by elevation zones, aspect classes, and glacierized/non-glacierized areas. The model has different routines: snow and glacier, soil, response, and routing. The melt in the snow and glacier routine is calculated with a degree-day method and a higher degree-day factor is used for glacier ice

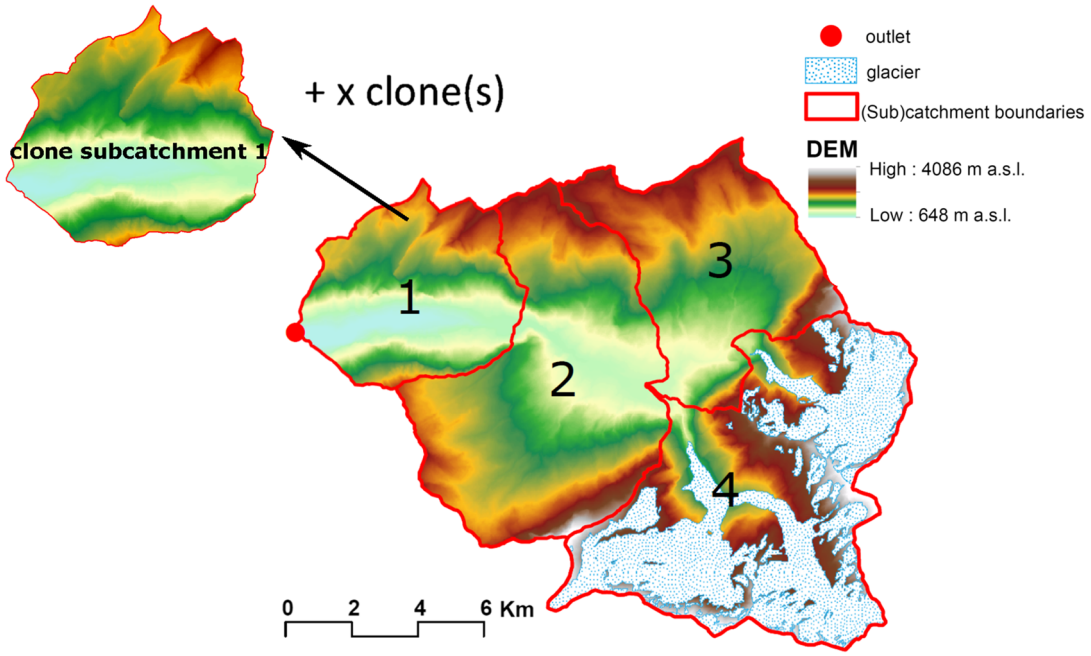

FIGURE 2 Base catchment used to create the virtual catchments for the model experiment. Numbers indicate the different subcatchments

TABLE 1 The nested model catchments with different relative glacier covers

Model catchments	Glacier cover	Subcatchments included	Clone(s) of subcatchment 1 added	Mean elevation (m a.s.l.)
Original				
g_{orig}	20.1%	1, 2, 3, 4	0	2058
Decreased glacier cover				
g_{15}	15.2%	1, 2, 3, 4	2	1908
g_{10}	10.2%	1, 2, 3, 4	6	1756
g_{5}	5.1%	1, 2, 3, 4	18	1603
g_{3}	3%	1, 2, 3, 4	35	1539
g_{1}	1%	1, 2, 3, 4	117	1478
Increased glacier cover				
g_{24}	24%	2, 3, 4	0	2176
g_{37}	37.2%	3, 4	0	2413
g_{57}	57.2%	4	0	2703
Extreme glacier covers				
g_{0}	0%	1, 2, 3, 4	117	1478
g_{100}	100%	Part of 4	0	2819

compared with snow. The model simulates discharge in daily time-steps (Q) and also calculates the streamflow originating from the glacierized (Q_{gl}) and the non-glacierized part (Q_{nongl}) of the catchments, so that

$$Q = Q_{gl} + Q_{nongl}$$

whereby Q_{gl} includes streamflow from rain, snowmelt, and ice melt, and Q_{nongl} includes streamflow from rain and snow melt. For a detailed model description, we refer to Seibert and Vis (2012) and Seibert et al. (2018).

The model settings are based on Stahl et al. (2017) and Meyer et al. (2019), who modelled the original catchment as one of the headwater catchments of the river Rhine. Catchment model settings (elevation zones, aspect classes, and glacierized and non-glacierized area fractions) were calculated for each of the nested model catchments. The model for each of the nested catchments was forced with the same daily temperature (T) and precipitation (P) data (representative for the mean elevation of the original catchment) from Meteoswiss (RhiresD and TabsD gridded products, MeteoSwiss, 2013, 2016), with T and P corrected for elevation according to a gradient. Mean annual precipitation sums range from 1,456 mm for the lowest to 2,211 mm

for the highest catchment. Parameters were taken from Meyer et al. (2019), who calibrated the model on multiple criteria, including streamflow data, estimated glacier volumes, and on a gridded snow water equivalent product from SLF (Swiss WSL-institute for Snow and Avalanche Research). Streamflow was modelled for the period 1976–2015, and the glacier area was kept constant during the simulation of this period for each modelled catchment.

2.2 | Multi-catchment data set

The relationship between CV_Q and g from the modelled nested catchments was compared with the relationship obtained from streamflow observations of 39 gauged catchments in the Swiss and Austrian Alps (Table A1, Figure 3). All catchments are situated at approximately the same latitude, but they are distributed from west to east over the Alps. Their g range from 0% to 73.5%, based on outlines for the year 2010 and 2012 for Switzerland and Austria, respectively (Table 2). For reference, the data set also contains four Swiss non-glacierized catchments.

Most catchment areas are between 10 and 100 km^2 with some larger ones between 200 and 517 km^2. The mean elevation is around 2,000–2,500 m a.s.l. for the glacierized and around 1,000–1,500 m a.s.l. for the non-glacierized catchments. The highest catchment (3,122 m a.s.l. mean elevation) is the Vernagtbach catchment in Austria, which also has the highest glacier cover and is one of the smallest catchments. In a few catchments, the elevation range is more than 2,500 m (see Table A1). Glacier area ranges from smaller than 1 km^2 to larger than 100 km^2.

Mean annual precipitation sums in the catchments range from 940 mm to more than 2,300 mm. Precipitation is highest in summer for all catchments, with a second smaller peak around November. Monthly mean temperatures are in general above 0°C between May and October for the glacierized catchments and only below 0°C in winter (December–February) for the non-glacierized catchments. Mean annual temperatures are higher for the non-glacierized catchments because of their lower elevation. Daily P and T data are taken from interpolated observations: the SPARTACUS gridded product (1 × 1 km, Hiebl & Frei, 2016, 2018) for Austria and the RhiresD (~1×1 km, precipitation) and TabsD (~1×1 km, temperature) gridded products (MeteoSwiss, 2013, 2016) for Switzerland.

All streamflow records have a length of at least 40 years (one selection criterion for catchments was that streamflow time series cover the period 1976–2015). Some of the Swiss catchments have streamflow records starting already before 1950. Daily streamflow data were obtained from the FOEN (Swiss Federal Office for the Environment) and from the eHYD database from the Austrian Federal Ministry Sustainability and Tourism (https://ehyd.gv.at/). Daily data for the Vernagtbach (Austria) were available for summer (May–October) days only and winter data were infilled with the same mean monthly data every winter from Escher-Vetter, Braun, and Siebers

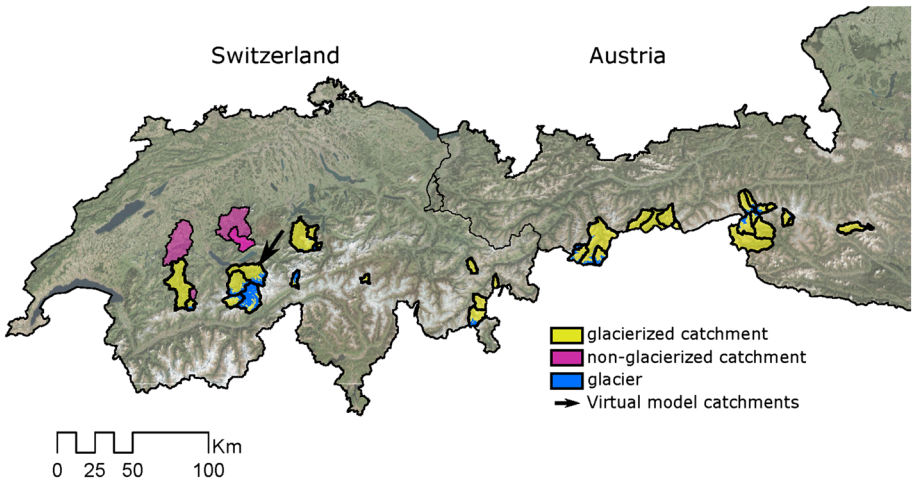

FIGURE 3 Location of the study catchments in Switzerland and Austria. The arrow shows the location of the catchment that was used as basis for the model experiment. This catchment was not part of the multicatchment analysis

TABLE 2 Glacier outline data sets and their references for Switzerland and Austria

Switzerland		Austria	
g inventory year	Reference	*g* inventory year	Reference
1935	Freudiger, Mennekes, Seibert, & Weiler, 2018	1969, 2006	Fischer, Seiser, Stocker-Waldhuber, Mitterer, & Abermann, 2015
1973	Müller, Caflish, & Müller, 1977; Maisch, Wipf, Denneler, Battaglia, & Benz, 2000	2012	CORINE land cover data
2003	Paul, Frey, & Le Bris, 2011		
2010	Fischer, Huss, Barboux, & Hoelzle, 2014		

(2014) who found a low winter variability based on a few stage measurement campaigns (Escher-Vetter & Siebers, 2014). Two records had gaps of two and three years of data, respectively (in the period 1976–2015). These years were excluded from the analysis for these catchments. All streamflow records are assumed to be undisturbed. However, two catchments are flagged by the FOEN as influenced (e.g., by subdaily hydropeaking; see Table A1). As no typical hydropeaking signal or other disturbance signal was evident in the daily streamflow time series, we assumed that the influence is negligible with the monthly and annual time resolutions used in this study.

2.3 | Analysis of streamflow variability

The coefficient of variation (CV)

$$CV_Q = \frac{\sigma}{\mu},$$

was used as metric for interannual streamflow variability (Chen & Ohmura, 1990; Fountain & Tangborn, 1985). CV_Q was calculated for yearly values of annual streamflow (Q_{ann}) and August streamflow (Q_{aug}). August was selected because it can be assumed to be the month with highest ice melt because seasonal snow has melted from the glacier surface (Jost, Moore, Menounos, & Wheate, 2012; Lang, 1973; Stahl & Moore, 2006), although some studies also found September to be the month with highest glacier melt contribution (e.g., Frans, Istanbulluoglu, Lettenmaier, Fountain, & Riedel, 2018). CV_Q was plotted against g to test for the presence of a GCE curve (Figure 1). Leap days were removed before aggregating daily streamflow series. Only streamflow sums from years or months without any data gaps were considered. CV_Q was calculated for the period 1976–2015 both for the model experiment and the multicatchment data set.

To analyse the potential controls on the GCE curve (see Introduction) and GCE_{opt}, we examined how streamflow variability relates to precipitation and temperature variability, by calculating the Spearman correlation coefficient between streamflow and the two climate variables (r_{P-Q}, r_{T-Q}). Correlation coefficients were calculated for all catchments from the model experiment and the multi-catchment data set for the same period as CV_Q (1976–2015).

2.4 | Time stability of GCE curve

For some of the Swiss catchments in the multi-catchment data set, long time series are available (>40 years). For a selection of those, CV_Q was calculated for different subperiods (see Table A1). The definition of the subperiods was based on the reference years of available g data. We used the glacier outline data sets of 1935, 1973, and 2003 (Table 2). The corresponding 20-year subperiods to derive CV_Q were 1932–1951, 1965–1984, and 1996–2015. Plotting, for each catchment, the CV_Q of the subperiods against the g of the subperiods shows whether changes in g over time lead to expected changes in CV_Q (following the curve, decreasing, or increasing CV_Q). Furthermore, we also tested how stable the relationship is in time by calculating CV_Q for two 20-year periods (1965–1984 and 1996–2015 for the multi-catchment data set, 1976–1995 and 1996–2015 for the model experiment) and relating them to the g values from the available glacier inventories in 1969 and 2006 for Austria and 1973 and 2003 for Switzerland. Then, a second-order polynomial was fitted, as suggested by Chen and Ohmura (1990), and compared for the two periods. Also here, the three to five gap years in three of the catchments in the different analyses periods were excluded from the analyses.

3 | RESULTS

3.1 | Model experiment

The CV_Q values of the virtual nested catchments show a convex relationship with g (Figure 4a,b). The GCE curve optimum lies around g = 15% for Q_{ann} and around g = 10% for Q_{aug}. CV_Q is generally higher for Q_{aug} than for Q_{ann}, especially at high and low g. The CV_Q of the g_{100} catchment shows some deviation from a smooth curve. The correlations of streamflow with precipitation and temperature cross at g 15–20% for Q_{ann} and at g 10–15% for Q_{aug}, which corresponds with the optimum in the GCE curve (Figure 4c,d). As expected, streamflow of catchments with high g correlates more strongly with temperature than with precipitation, for the low g catchments it is opposite. With increasing g, the increase/decrease of the correlations levels off. The anomalies of the two streamflow components Q_{gl} and Q_{nongl} (standard deviation shown in Figure 4e,f) are of the same magnitude around GCE_{opt}. The 1:1 ratio of the two streamflow components is found between g 24% and 37.2% for Q_{ann} and at g = 15% for Q_{aug} (Figure 4g,h). Although the magnitude of the component and the magnitude of the component anomaly are related, they show a 1:1 ratio at different g. The ratios show higher values for Q_{aug}, indicating that compared with the whole year, Q_{gl} is a more important contributor to total streamflow in August.

Figure 5 illustrates the compensating effect by showing the anomalies of the streamflow components Q_{gl} and Q_{nongl} per year. In catchments with g lower than the optimum (g_{10} and g_3, Figure 5, left column), the Q_{nongl} anomalies are larger than the Q_{gl} anomalies. A negative anomaly in Q_{nongl}, for example, due to a precipitation deficit, cannot be offset by a positive anomaly in Q_{gl} because Q_{gl} is not large enough. On the other hand, for catchments with g above the optimum (g_{37} and g_{20}, Figure 5, right column), the Q_{gl} anomalies are much larger than those of Q_{nongl} and, therefore, they can also not counterbalance each other. At g near the GCE curve optimum (g_{15} and g_{10}, Figure 5, middle column), the Q_{gl} and Q_{nongl} anomalies are similar. Besides being of comparable magnitude, the direction of the anomalies should also be opposite to counterbalance each other. In most years, this is the case (e.g., 1977, 1978), but sometimes the anomalies have the same sign (e.g., 1996 for Q_{ann}). Total streamflow (Figure 5) shows the effect of the interplay of the two components. For example, at low g, Q_{ann} and Q_{aug} are mostly determined by anomalies in Q_{nongl}, but in

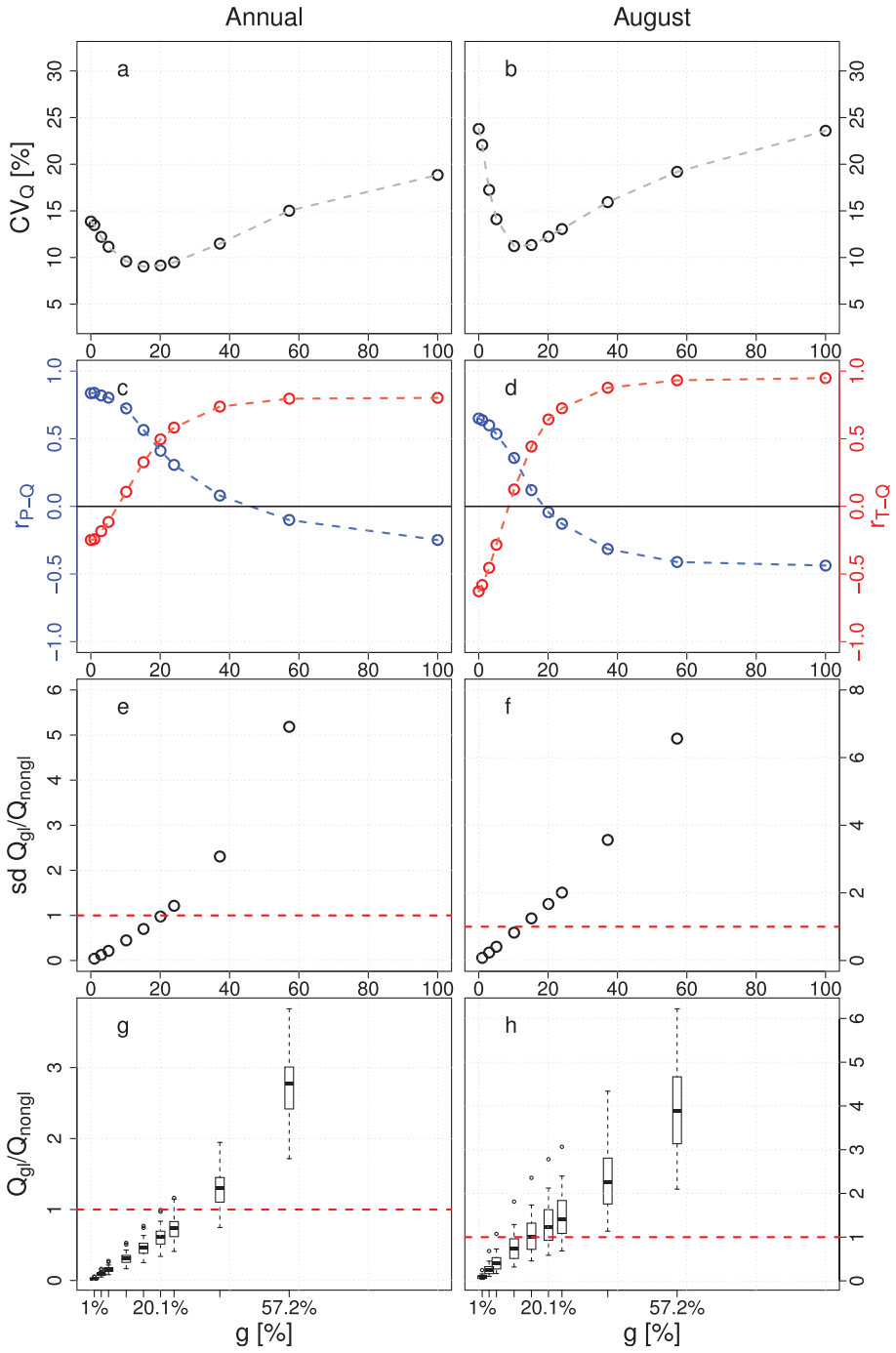

FIGURE 4 GCE curve, its drivers, and the streamflow components obtained from the simulations of the nested model catchments. Left column is Q_{ann}, right column Q_{aug}. (a) and (b) show the relation between *g* and CV_Q, (c) and (d) the correlations $r_{T\text{-}Q}$ (red) and $r_{P\text{-}Q}$ (blue), (e) and (f) the ratio of the standard deviation of the streamflow components Q_{gl} and Q_{nongl}, and (g) and (h) show the ratio of total Q_{gl} and Q_{nongl} in boxplots (data of all years). The dashed lines in a, b, c, and d connect the results from the different catchments

years when Q_{gl} is more substantial and opposite to Q_{nongl}, total streamflow is closer to the mean streamflow. Near GCE_{opt}, total streamflow shows large deviations when the anomalies have the same sign and close to average values when the anomalies are opposite.

3.2 | Multi-catchment empirical analysis

Figure 6 shows the same type of analysis as in Figure 4a–d, but now for the observed streamflow records from the multicatchment data set instead of the modelled nested catchments. In general, the CV_Q of observed streamflow is higher than the modelled CV_Q (dashed line). The CV_Q of the multicatchment data set shows a scatter, and it is difficult to find a clear curve with an optimum. For Q_{ann}, CV_Q decreases with increasing *g* between 0% and 15%. This part of the graph is, however, dominated by the four non-glacierized catchments showing high CV_Q (Figure 6a,b). There are not many catchments with a high *g*. The Vernagtbach catchment (with highest *g*, 73.5%) is an important data point to indicate a potential increase in CV_Q going from moderate to high *g*, especially for Q_{ann}. However, its data are uncertain for Q_{ann}, due to the infilling of mean winter streamflow values. For both Q_{ann} and Q_{aug},

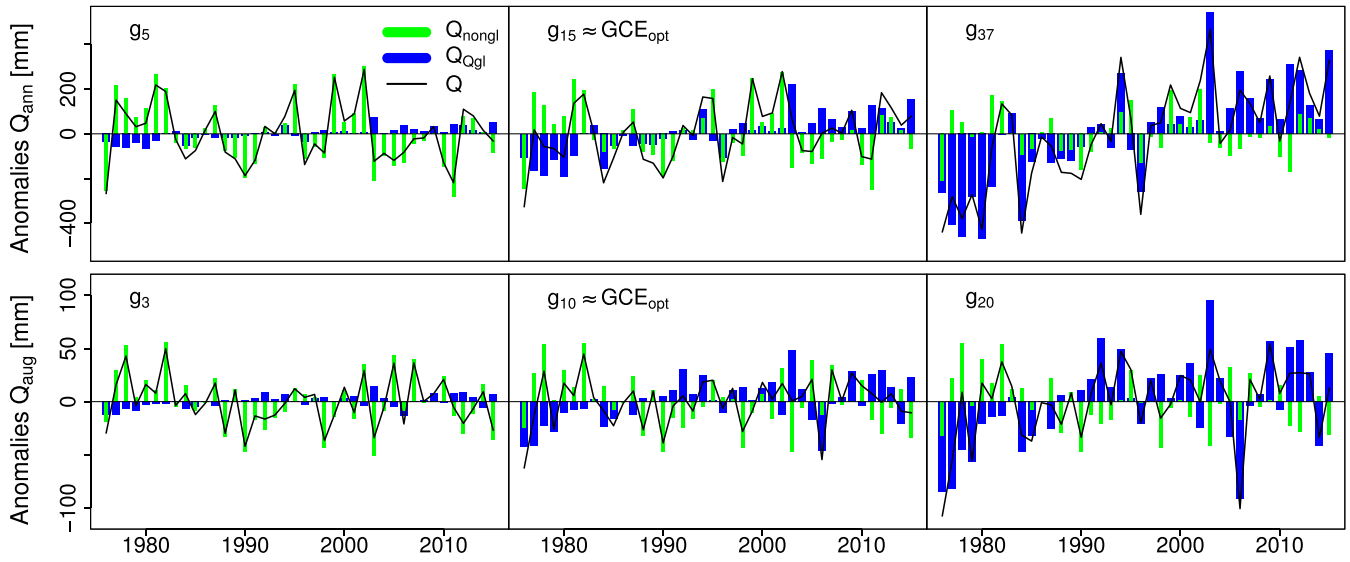

FIGURE 5 Streamflow anomalies of the modelled Q_{ann} (upper) and Q_{aug} (lower) streamflow components. Anomalies of Q_{nongl} are shown in green, anomalies of Q_{gl} in blue, and anomalies of total streamflow are shown as black line. Anomalies are shown for a catchment close to the GCE optimum (middle), left of the optimum (left column), and right of the optimum (right column), based on Figure 4a and b. Anomalies are calculated for the components and the total streamflow as deviations from the Q_{gl}, Q_{nongl}, and Q mean of 1976–2015

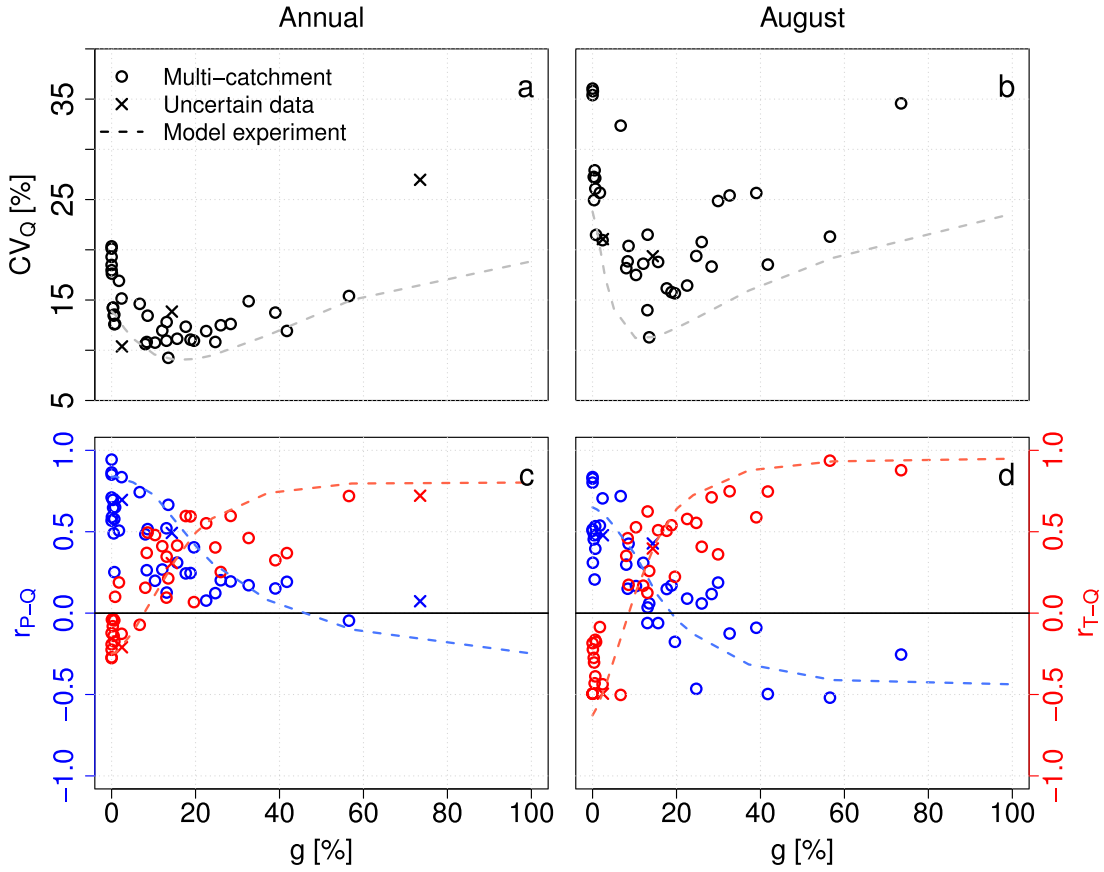

FIGURE 6 Relation between *g* and CV_Q (a,b) and the correlations $r_{T\text{-}Q}$ (red) and $r_{P\text{-}Q}$ (blue) (c,d) for the multicatchment data set. Left column shows results for Q_{ann}, right column for Q_{aug}. Crosses indicate uncertain data (hydropeaking and infilled winter streamflow). For comparison, dashed lines correspond to lines derived from the results of the nested model catchment experiment as shown in Figure 4a–d

the Vernagtbach catchment shows a much higher CV_Q compared with the model experiment. For Q_{aug}, the decrease and subsequent increase in CV_Q from non- to high-glacierized catchments is more evident than for Q_{ann}, but the scatter near the modelled optimum is large. The correlations of streamflow with precipitation and temperature, $r_{P\text{-}Q}$ and $r_{T\text{-}Q}$, are more comparable to the model results.

The crossing of the correlations is present, although again, there is a scatter. The observations show a range of g where $r_{P\text{-}Q}$ and $r_{T\text{-}Q}$ have approximately the same value rather than one crossover point. This range is narrower for Q_{aug} than for Q_{ann}. The few catchments with g < 1% show a larger range of correlation values than that were modelled for the two nested catchments with lowest g, g_0, and g_1.

3.3 | Changes of streamflow variability over time

Another test of the GCE curve theory is to see if CV_Q changes over time follow the expected curve pattern. Few series are long enough to study changes in time, and in those catchments, g changes over time (x-axis) are rather small and none of the changes represent a large part of the entire GCE curve (Figure 7), although g is decreasing over time for all catchments. The CV_Q of Q_{ann} of the 20-year periods for the selected catchments are closer to the GCE curve from the model experiment than the CV_Q values resulting from the 40-year analysis for the complete multicatchment data set (Figure 6a), which were distinctly higher. Most of the changes over time for Q_{ann} broadly follow the shape of the curve in terms of decreasing/increasing CV_Q, apart from the catchment with lowest g and the catchment around the optimum g. For Q_{aug}, the two highest glacierized catchments also show different patterns (Figure 7). However, the different catchments cannot be connected by an ideal curve because they have very different CV_Q or different rates of change of CV_Q (different slopes). The catchment closest to the modelled GCE_{opt} (black line in Figure 7) shows a reversed pattern of the GCE curve because instead of decreasing and then increasing CV_Q when passing the optimum g, the data shows increasing and then decreasing CV_Q. Most of the catchments show a different trend in CV_Q for Q_{ann} compared with Q_{aug}.

Using a larger subsample of the multicatchment data-set and fitting a second-order polynomial through the data points, as done by Chen and Ohmura (1990), result in very different curves for different time periods (Figure 8, left). The curve for the later period, 1996–2015, agrees most with the curve from Chen and Ohmura (1990), although in their study data from years until 1985 were used. Moreover, especially the earlier period, 1965–1984, shows that a second-order polynomial might not be the best function to describe the relation between CV_Q and g. Also in the model experiment, the fitted curves differ between the two periods (Figure 8b). The later period, 1996–2015, shows lower CV_Q for the moderate- to high-glacierized catchments compared with the earlier period, 1976–2015.

4 | DISCUSSION

4.1 | Is there a universal relationship between glacier cover and interannual streamflow variability?

The model experiment confirmed the hypothesis of a convex relationship between g and CV_Q (Figure 4). In a controlled nested catchment setting, glacier cover thus influences streamflow variability. The left part of the curve (where rainfall–runoff regimes are dominant) was steeper than the right part (where melt regimes are dominant), more so for August streamflow. This suggests that precipitation and temperature may influence the streamflow variability differently and is broadly consistent with the asymmetric behaviour found for correlations of streamflow with precipitation and temperature. Results of this model experiment, however, do not support the simple quadratic shape of the GCE curve suggested by Chen and Ohmura (1990) for the Alps. The multicatchment data set had overall higher CV_Q than the modelled virtual catchments; the modelled GCE curve appears to represent a lower envelope of the multicatchment CV_Q. This is possibly due to the general tendency of underestimation of streamflow variability, including extremes, by a model (e.g., Whitfield, Wang, & Cannon, 2003) and due to our idealized nested catchment model framework in which, for example, parameters do not change with

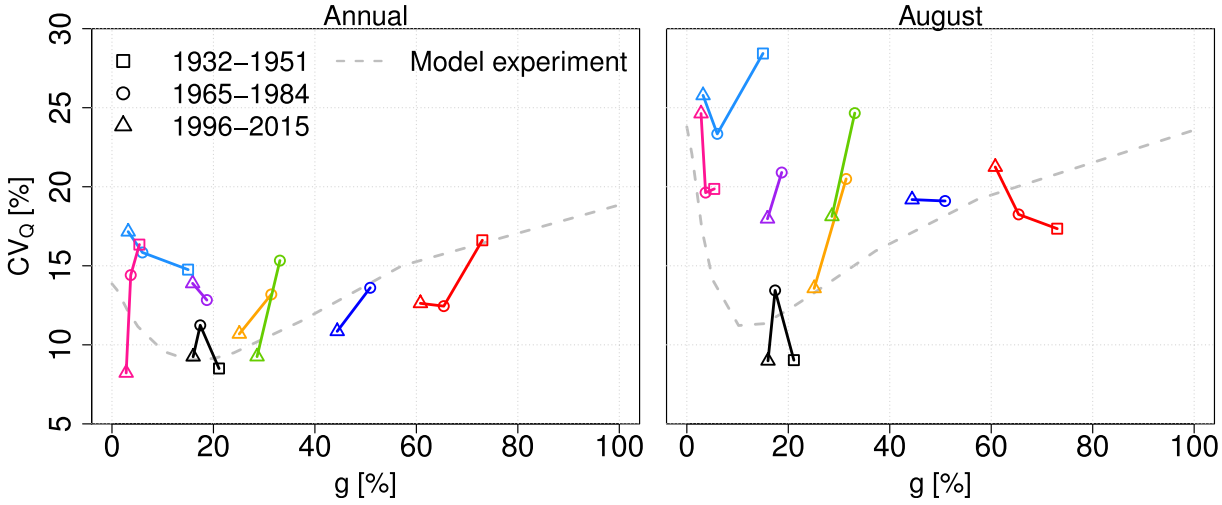

FIGURE 7 CV_Q of Q_{ann} (left) and Q_{aug} (right) for three 20-year time windows around glacier cover inventory dates (different symbols) for eight Swiss catchments (different colours) with long observed streamflow time series. The dashed grey curve in the background is from the model experiment as shown in Figure 4a and b

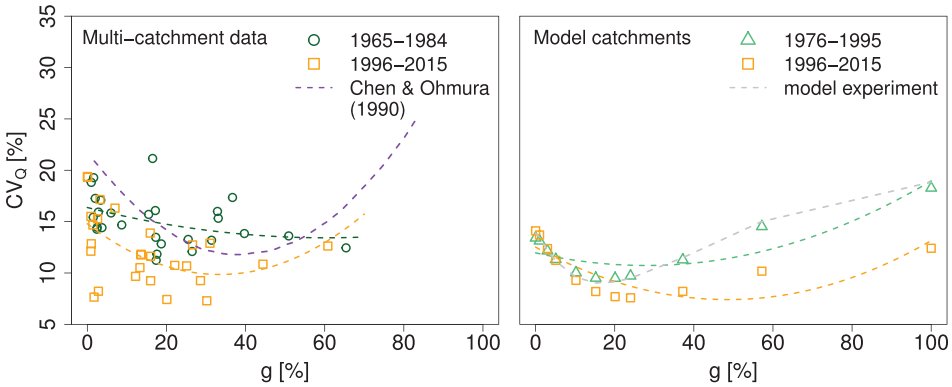

FIGURE 8 Relation between CV_Q and g for different 20-year time periods for Q_{ann}. Left shows the multicatchment data set, right the nested model catchments. A second-order polynomial was fitted through the points. Only catchments that have streamflow data for both periods were used. The curve from Chen and Ohmura (1990) is plotted for comparison in the left panel. In the right panel, the GCE curve from the model experiment (40-year data) is shown in grey

catchment size, glaciers are modelled statically, and other simplifications. The scatter was high and the multicatchment data set did only roughly show a GCE curve (Figure 6). Decreasing streamflow variability with increasing g in the low-glacierized part was evident for Q_{ann} and Q_{aug}. At the GCE_{opt} of the model experiment for Q_{aug}, the multicatchment data set showed a large range of CV_Q. An increase in CV_Q to the right of an assumed optimum was less evident and depended strongly on one data point for the catchment with the highest glacier cover (73.5% Vernagtbach), which has infilled streamflow data in winter due to discontinuous streamflow monitoring.

In the multicatchment data set and the model experiment, the correlations with climate drivers showed a crossover. From low- to high-glacierized catchments, the correlation of streamflow with precipitation decreased, whereas the correlation with temperature increased. However, only in the model experiments, due to the clear GCE curve, the crossover of correlations could be clearly related to the optimum in the GCE curve. In the multicatchment data set, a similar correlation in r_{P-Q} might have resulted in different CV_Q because of variations in, for example, mean streamflow or magnitude of streamflow anomalies due to dissimilarity in storage characteristics. Also, glacier characteristics can vary with respect to, for example, their water retention capacity (e.g., Jansson et al., 2003; Hock et al., 2005) or aspect (e.g., Hock, 2003, 2005), which influences the balance of Q_{gl} and Q_{nongl} on shorter or longer timescales and could cause the scatter in the CV_Q and r_{P-Q} and r_{T-Q} for catchments with similar g. The correlations might therefore only be a very rough indicator of a catchment's location relative to the GCE optimum.

We showed that a universal relationship between CV_Q and g in the Alps that could be used for quantitative planning does not exist. A space-for-time interpretation of the curves postulated by Chen and Ohmura (1990) and Fountain and Tangborn (1985) is not advised based on our analyses for two reasons: (a) In our intraregional analysis of streamflow observations, we could not find a distinct relation between CV_Q and g following a theoretical GCE curve, and (b) changes over time of CV_Q do not follow one common curve and also the relation itself is not stable over time. Possible reasons for the differences between our study and Chen and Ohmura (1990) could be the different time periods analysed. We chose a common period for all catchments (1976–2015), whereas Chen and Ohmura (1990) took different lengths of time series as available for the different catchments. If a different time period had caused the different results, this would mean that the relationship is not stable over time. However, redoing the exact same analyses as Chen and Ohmura (1990) with the same catchments for the same period, we found that some catchments were apparently not included in the fit of the curve given by Chen and Ohmura (1990) although being mentioned in their paper (Figure 9). We do not know the reason for leaving those out, but it might have influenced the results.

Relative glacier cover might not be the best indicator of the balance between the two runoff regimes in a partly glacierized

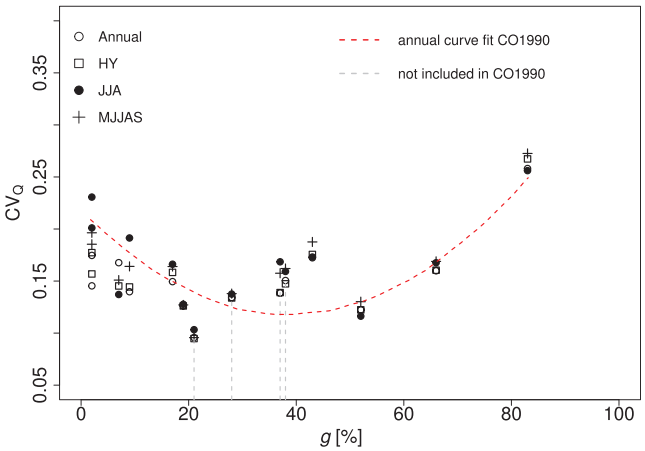

FIGURE 9 Reconstruction of the GCE curve by Chen and Ohmura (1990). Overlapping catchments in our study with Chen and Ohmura (1990) were plotted for the same time period. CV_Q was calculated for annual streamflow, Hydrological years (HY), summer months June, July and August (JJA), and summer half year (MJJAS). CV_Q is expressed as fraction, not percentage. Grey lines indicate catchments that were listed in the data section of Chen and Ohmura (1990) but not included in the figure of the quadratic fit

catchment. When glaciers melt due to warming, they may thin, the snow and firn reservoirs on the glaciers may reduce, and the accumulation ablation ratio can change (e.g., Dyurgerov, 2003; Paul, Kääb, & Haeberli, 2007), all before notable decreases in g occur. These changes, however, could influence the amount of Q_{gl}. These processes might play a role when comparing different catchments with similar g and when analysing changes over time for a particular catchment. Thus, also the balance of the glacier with climate can influence the GCE. A more balanced glacier has a different Q_{gl} component than a glacier that is out of balance (e.g., Pritchard, 2019). European glaciers experienced close to balanced conditions around 1960–1980 (e.g., Vincent et al., 2017). The period analysed in Chen and Ohmura (1990) mostly covers this rather stable period, whereas the more recent period used in this study (1976–2015) is characterized by negative mass balances and retreating glaciers (Huss, Bauder, Funk, & Hock, 2008).

Our results correspond to some earlier studies. Farinotti, Usselmann, Huss, Bauder, and Funk (2012) also found no clear pattern of CV_Q and g when modelling streamflow of several glacierized catchments for 1900–2100, allowing glaciers to retreat, and considering aggregated results for all catchments. Zhang et al. (2016) also found no quadratic GCE relationship, but instead plotted a power law function through 24 catchments in the Tian Shan Mountains. The results of Collins (2006b) for deglaciating catchments in the Alps show similar patterns compared with some of the selected Swiss catchments with long time series in our study (Figure 7). Comparing the streamflow of 1956–1980 with 1981–2005, he found an increase in CV_Q for catchments with a high g and a decrease for catchments with a low g, which contradicts a GCE curve pattern. Our data showed a shift in the y-values of the GCE curve over time, especially for the modelled catchments (Figure 8, right), but also a shift of GCE_{opt} (x-axis) might be possible if the Q_{gl} component becomes more dominant without a change in g. This could happen, for example, if rainfall in the non-glacierized part decreases, or if there will be less snow cover on the glacier. Both potential directions of change of the relationship strongly limit its use for planning and indicate that processes involved in the glacier compensation effect are complex.

4.2 | Limitations and other controls on GCE

The multicatchment analyses as well as the model experiment revealed a number of limitations for the analysis of GCE. For example, undisturbed streamflow observations from high-glacierized catchments are rare. Such data are, however, important for analysing the right part of a potential GCE curve, particularly the steepness of this part of the curve. The Vernagtbach catchment (g = 73.5%) proved its importance in our analysis, as well as in the study of Chen and Ohmura (1990), but it might be a unique catchment due to its small elevation range and a glacier that has retreated to a half-circle shape (with different aspects) and that has known surging behaviour (Hoinkes, 1969). Furthermore, the lack of observations of glacier cover at different historical times limits the combined analyses with long streamflow records.

In the study area, observed decreases in g over the time periods covered by streamflow and glacier area observations are rather small (in the order of 5–10%). That makes it difficult to attribute changes in observed streamflow variability to changes in glacier cover. The few catchments with long time series only represent a small part of the theoretical curve. Glaciers adjust their size and elevation distribution to be in balance with climate, that is, in a warming climate, they retreat to higher elevations. These adjustments affect Q_{gl} and Q_{nongl}, and the GCE may depend on glacier mass balance and on the phase of peak glacier melt water (e.g., Huss & Hock, 2018; Immerzeel, Pellicciotti, & Bierkens, 2013). Another modelling experiment would be needed to analyse how the streamflow variability of (different) high-glacierized catchments develops over time when the glacier is retreating and even disappears (and the climate is changing)(e.g., Hagg, Braun, Kuhn, & Nesgaard, 2006; Nolin, Phillippe, Jefferson, & Lewis, 2010). Our results suggest that each catchment may have an individual GCE curve (Figure 7) with a different optimum and a different level of CV_Q values. However, during glacier retreat, even the temporal trajectories of individual catchments may not follow a fixed GCE curve due to simultaneous changes in glacio-hydrological processes and climate characteristics.

It is important to note that total streamflow in the model experiment was separated in streamflow components from the glacierized and the non-glacierized part (Figures 4 and 5) but with runoff from snowmelt included in both. Snow depends both on precipitation (deposition) and temperature (melt), so it influences the non-glacierized part and the glacierized part of the catchment. Collins (2006a, 2006b) and Moore (1992) discuss the importance of the interannual variability of snow on the GCE. In warm summers following dry winters, the snow line rises sooner and higher up-glacier, allowing more ice to melt over a larger area compared with years with cool (or also warm) summers following snowy winters. In addition, in long time series of streamflow, not only relative glacier cover can change but also the area of bare ice when the snow line rises transiently (Collins, 2006b; Dahlke, Lyon, Jansson, Karlin, & Rosqvist, 2014; Hock et al., 2005). Thus, the role of snow in the GCE is complicated. Further studies addressing particularly the role of snow within the GCE context could give more insights in the interannual streamflow variability that is not explained by glacier cover alone.

We explored potential relations with some other catchment characteristics that may explain the variability in the empirical relations of CV_Q values with g (Figures S1 and S2). Elevation characteristics, temperature, and catchment area showed some effect on CV_Q. Mean elevation and temperature are however also related to g. Further model experiments and sensitivity analyses could give insights in the importance of other characteristics on streamflow variability in glacierized catchments, if models are able to represent hydrological (e.g., evapotranspiration and groundwater storage) and glaciological processes (glacier dynamics) in glacierized and non-glacierized catchments well.

Besides snow and catchment characteristics, antecedent conditions (for monthly flows) and changes and/or differences in climate characteristics might also be relevant to take into account. Annual

mean temperature has been increasing over our analysed period, and precipitation amounts have been rather stable or slightly increasing. However, the variability of T and P was fluctuating over time. If these fluctuations are large, glacier cover cannot compensate for them and changes in CV_Q are then not only glacier cover related but also climate related (Collins, 2006a; Fleming et al., 2006). Another aspect of climate that could be important is the type of summer weather (Casassa et al., 2009; Moore, 1992). Moore (1992) suggests that in catchments with dry summers, in contrast to catchments with wet summers, the negative correlation between Q_{gl} and Q_{nongl} is more pronounced. In the Alps, the catchments have wetter summers compared with the summers in coastal North America, where most of the other studies on streamflow variability were conducted (e.g., Fleming & Clarke, 2005; Fountain & Tangborn, 1985; Moore, 1992). Combining different climatic influences within one regional sample may obscure a clear GCE curve. In our analysis, precipitation seasonality is similar for all catchments, but the relatively wet summers and varying precipitation amounts might complicate the search for a GCE curve. Related to that is the question of how the GCE appears in unstudied climates with distinctly differing amounts of precipitation and glacier melt and their interaction, possibly resulting in a different shape of a GCE curve. Moreover, we might need to think of a relationship for the compensating effect of glaciers that also includes climate characteristics on the axes (like the Budyko curve) to be robust for changes in climate that are not only influencing *g*, and to distinguish different climates. Such a relationship would then better allow for space-for-time substitution interpretations.

5 | CONCLUSION

This study analysed the potential to identify a universal relationship between glacier cover and interannual streamflow variability using complementary analyses of empirical data and a model experiment. The nested catchment model experiment resulted in a characteristic convex GCE curve confirming the theory that streamflow variability is dependent on relative glacier cover. In this idealized case, the relative glacier cover determines if precipitation or temperature dominates streamflow variability as shown by the correlation of streamflow with precipitation and temperature. The optimum glacier cover corresponding to the lowest interannual streamflow variability derived from the model experiment was around 10% or 15% glacier cover, for annual and August streamflow, respectively. In contrast, the empirical analysis based on real observations from a multicatchment data set showed a considerable scatter, especially the hypothesized increased streamflow variability with increasing glacier cover was not evident.

Comparing the GCE curve from the multicatchment data with that from the model experiment shows that relative glacier cover does not completely overrule other factors that could influence streamflow variability, such as other catchment or glacier characteristics. This means that a relationship fitted to data from some (modelled) catchments cannot be transferred to catchments with other characteristics. Our results also showed that the relationship between glacier cover and interannual streamflow variability can change over time and that individual catchments do not clearly follow one curve over time. Differences between our results and previously published relationships shed doubt on the existence of an ideal and simple universal relationship between streamflow variability of different catchments with different glacier cover and therefore on the validity of the use of such a GCE curve for estimating streamflow variability in glacierized catchments. Consequently, one needs to be careful about generalizing the role of glaciers as ideal buffers and assuming a characteristic GCE curve that can directly be used for space-for-time substitution applications.

DATA AVAILABILITY STATEMENT

Streamflow data from Austria are openly available from the eHYD database at https://ehyd.gv.at/. Swiss streamflow data were provided by the Swiss Federal Office for the Environment (FOEN) and available there on request. Climate data were made available by Zentralanstalt für Meteorologie und Geodynamik (ZAMG) and Meteoswiss, for Austria and Switzerland, respectively and are available on request from these institutions. Data were used under license for this project and study. Glacier outline data are available according to the given references.

ORCID

Marit van Tiel https://orcid.org/0000-0002-4819-337X
Irene Kohn https://orcid.org/0000-0002-8099-867X
Anne F. Van Loon https://orcid.org/0000-0003-2308-0392
Kerstin Stahl https://orcid.org/0000-0002-2159-9441

REFERENCES

Andrés Doménech, I., García Bartual, R. L., Montanari, A., Segura, M., & Bautista, J. (2015). Climate and hydrological variability: The catchment filtering role. *Hydrology and Earth System Sciences*, *19*(1), 379–387. https://doi.org/10.5194/hess-19-379-2015

Barlow, M., Nigam, S., & Berbery, E. H. (2001). ENSO, Pacific decadal variability, and US summertime precipitation, drought, and stream flow. *Journal of Climate*, *14*(9), 2105–2128. https://doi.org/10.1175/1520-0442(2001)014<2105:EPDVAU>2.0.CO;2

Braithwaite, R. J., & Olesen, O. B. (1988). Effect of glaciers on annual runoff, Johan Dahl Land, south Greenland. *Journal of Glaciology*, *34*(117), 200–207. https://doi.org/10.3189/S002214300003224X

Carmona, A. M., Sivapalan, M., Yaeger, M. A., & Poveda, G. (2014). Regional patterns of interannual variability of catchment water balances across the continental US: A Budyko framework. *Water Resources Research*, *50*(12), 9177–9193. https://doi.org/10.1002/2014WR016013

Casassa, G., López, P., Pouyaud, B., & Escobar, F. (2009). Detection of changes in glacial run-off in Alpine basins: Examples from North America, the Alps, central Asia and the Andes. *Hydrological Processes: An International Journal*, *23*(1), 31–41. https://doi.org/10.1002/hyp.7194

Chen, J., & Ohmura, A. (1990). On the influence of Alpine glaciers on runoff. *IAHS Publication*, *193*, 117–125.

Collins, D. N. (2006a). Climatic variation and runoff in mountain basins with differing proportions of glacier cover. *Hydrology Research*, *37*(4-5), 315–326. https://doi.org/10.2166/nh.2006.017

Collins, D. N. (2006b). Variability of runoff from Alpine basins. *IAHS Publication*, *308*, 466.

Dahlke, H. E., Lyon, S. W., Stedinger, J. R., Rosqvist, G., & Jansson, P. (2012). Contrasting trends in floods for two sub-arctic catchments in northern Sweden – does glacier presence matter?*Hydrology and Earth System Sciences*, *16*(7), 2123–2141. https://doi.org/10.5194/hess-16-2123-2012

Dahlke, H. E., Lyon, S. W., Jansson, P., Karlin, T., & Rosqvist, G. (2014). Isotopic investigation of runoff generation in a glacierized catchment in northern Sweden. *Hydrological Processes*, *28*(3), 1383–1398. https://doi.org/10.1002/hyp.9668

Dettinger, M. D., & Diaz, H. F. (2000). Global characteristics of stream flow seasonality and variability. *Journal of Hydrometeorology*, *1*(4), 289–310. https://doi.org/10.1175/1525-7541(2000)001%3C0289:GCOSFS%3E2.0.CO;2

Dyurgerov, M. (2003). Mountain and subpolar glaciers show an increase in sensitivity to climate warming and intensification of the water cycle. *Journal of Hydrology*, *282*(1-4), 164–176. https://doi.org/10.1016/S0022-1694(03)00254-3

Escher-Vetter, H., Braun, L. N., Siebers, M., (2014). Monthly averages of discharge as recorded at the Vernagtbach station for the period 1974 to 2012. *PANGAEA*. https://doi.org/10.1594/PANGAEA.832432

Escher-Vetter, H., & Siebers, M. (2014). *Technical comments on the data records from the Vernagtbach station for the period 2002 to 2012*. PANGAEA: Bremerhaven.

Farinotti, D., Usselmann, S., Huss, M., Bauder, A., & Funk, M. (2012). Runoff evolution in the Swiss Alps: Projections for selected high-alpine catchments based on ENSEMBLES scenarios. *Hydrological Processes*, *26*(13), 1909–1924. https://doi.org/10.1002/hyp.8276

Fischer, A., Seiser, B., Stocker-Waldhuber, M., Mitterer, C., & Abermann, J. (2015): The Austrian Glacier Inventories GI 1 (1969), GI 2 (1998), GI 3 (2006), and GI LIA in ArcGIS (shapefile) format. PANGAEA. https://doi.org/10.1594/PANGAEA.844988, Supplement to: Fischer, A et al. (2015)). Tracing glacier changes in Austria from the Little Ice Age to the present using a lidar-based high-resolution glacier inventory in Austria. *The Cryosphere*, *9*(2), 753–766. https://doi.org/10.5194/tc-9-753-2015

Fischer, M., Huss, M., Barboux, C., & Hoelzle, M. (2014). The new Swiss Glacier Inventory SGI2010: Relevance of using high-resolution source data in areas dominated by very small glaciers. *Arctic, Antarctic, and Alpine Research*, *46*(4), 933–945. https://doi.org/10.1657/1938-4246-46.4.933

Fleming, S. W., & Clarke, G. K. (2005). Attenuation of high-frequency interannual streamflow variability by watershed glacial cover. *Journal of Hydraulic Engineering*, *131*(7), 615–618. https://doi.org/10.1061/(ASCE)0733-9429(2005)131:7(615

Fleming, S. W., & Dahlke, H. E. (2014). Modulation of linear and nonlinear hydroclimatic dynamics by mountain glaciers in Canada and Norway: Results from information-theoretic polynomial selection. *Canadian Water Resources Journal/Revue canadienne des ressources hydriques*, *39*(3), 324–341. https://doi.org/10.1080/07011784.2014.942164

Fleming, S. W., (Dan) Moore, R. D., & Clarke, G. K. C., (2006). Glacier-mediated streamflow teleconnections to the Arctic Oscillation. *International Journal of Climatology*, *26*(5), 619–636. https://doi.org/10.1002/joc.1273

Fountain, A. G., & Tangborn, W. V. (1985). The effect of glaciers on streamflow variations. *Water Resources Research*, *21*(4), 579–586. https://doi.org/10.1029/WR021i004p00579

Frans, C., Istanbulluoglu, E., Lettenmaier, D. P., Fountain, A. G., & Riedel, J. (2018). Glacier recession and the response of summer streamflow in the Pacific Northwest United States, 1960–2099. *Water Resources Research*, *54*(9), 6202–6225. https://doi.org/10.1029/2017WR021764

Freudiger, D., Mennekes, D., Seibert, J., & Weiler, M. (2018). Historical glacier outlines from digitized topographic maps of the Swiss Alps. *Earth System Science Data*, *10*(2), 805–814. https://doi.org/10.5194/essd-10-805-2018

Gaudard, L., Romerio, F., Dalla Valle, F., Gorret, R., Maran, S., Ravazzani, G., … Volonterio, M. (2014). Climate change impacts on hydropower in the Swiss and Italian Alps. *Science of the Total Environment*, *493*, 1211–1221. https://doi.org/10.1016/j.scitotenv.2013.10.012

Hagg, W., Braun, L. N., Kuhn, M., & Nesgaard, T. I. (2006). Modelling of hydrological response to climate change in glacierized Central Asian catchments. *Journal of Hydrology*, *332*(1), 40–53. https://doi.org/10.1016/j.jhydrol.2006.06.021

Hiebl, J., & Frei, C. (2016). Daily temperature grids for Austria since 1961—Concept, creation and applicability. *Theoretical and Applied Climatology*, *124*(1-2), 161–178. https://doi.org/10.1007/s00704-015-1411-4

Hiebl, J., & Frei, C. (2018). Daily precipitation grids for Austria since 1961—Development and evaluation of a spatial dataset for hydroclimatic monitoring and modelling. *Theoretical and Applied Climatology*, *132*(1-2), 327–345. https://doi.org/10.1007/s00704-017-2093-x

Hock, R. (2003). Temperature index melt modelling in mountain areas. *Journal of Hydrology*, *282*(1-4), 104–115. https://doi.org/10.1016/S0022-1694(03)00257-9

Hock, R. (2005). Glacier melt: A review of processes and their modelling. *Progress in Physical Geography*, *29*(3), 362–391. https://doi.org/10.1191/0309133305pp453ra

Hock, R., Jansson, P., & Braun, L. N. (2005). *Modelling the response of mountain glacier discharge to climate warming*. In *Global change and mountain regions*. (pp. 243–252). Dordrecht: Springer. https://doi.org/10.1007/1-4020-3508-X_25

Hoinkes, H. C. (1969). Surges of the Vernagtferner in the Ötztal Alps since 1599. *Canadian Journal of Earth Sciences*, *6*(4), 853–861. https://doi.org/10.1139/e69-086

Hopkinson, C., & Young, G. J. (1998). The effect of glacier wastage on the flow of the Bow River at Banff, Alberta, 1951–1993. *Hydrological Processes*, *12*(10-11), 1745–1762. https://doi.org/10.1002/(sici)1099-1085(199808/09)12:10/11<1745::aid-hyp692>3.3.co;2-j

Huss, M., Bauder, A., Funk, M., & Hock, R. (2008). Determination of the seasonal mass balance of four Alpine glaciers since 1865. *Journal of Geophysical Research - Earth Surface*, *113*(F1). https://doi.org/10.1029/2007jf000803

Huss, M., & Hock, R. (2018). Global-scale hydrological response to future glacier mass loss. *Nature Climate Change*, *8*(2), 135–140. https://doi.org/10.1038/s41558-017-0049-x

Immerzeel, W. W., Pellicciotti, F., & Bierkens, M. F. P. (2013). Rising river flows throughout the twenty-first century in two Himalayan glacierized watersheds. *Nature Geoscience*, *6*(9), 742–745. https://doi.org/10.1038/ngeo1896

Jansson, P., Hock, R., & Schneider, T. (2003). The concept of glacier storage: A review. *Journal of Hydrology*, *282*(1-4), 116–129. https://doi.org/10.1016/s0022-1694(03)00258-0

Jenicek, M., Seibert, J., Zappa, M., Staudinger, M., & Jonas, T. (2016). Importance of maximum snow accumulation for summer low flows in humid catchments. *Hydrology and Earth System Sciences*, *20*(2), 859–874. https://doi.org/10.5194/hess-20-859-2016

Jost, G., Moore, R. D., Menounos, B., & Wheate, R. (2012). Quantifying the contribution of glacier runoff to streamflow in the upper Columbia River Basin, Canada. *Hydrology and Earth System Sciences*, *16*(3), 849–860. https://doi.org/10.5194/hess-16-849-2012

Koboltschnig, G. R., Schöner, W., Holzmann, H., & Zappa, M. (2009). Glaciermelt of a small basin contributing to runoff under the extreme climate conditions in the summer of 2003. *Hydrological Processes: An International Journal*, *23*(7), 1010–1018. https://doi.org/10.1002/hyp.7203

Krimmel, R. M., & Tangborn, W. V. (1974). South Cascade Glacier: The moderating effect of glaciers on runoff. *Proceedings of Western Snow conference, 42d Anchorage*, 9-13

Lang, H. (1973). *Variations in the relation between glacier discharge and meteorological elements* (pp. 85–94). ETH Zuerich: Versuchsanstalt fuer wasserbau, Hydrologie und Glaziologie.

Maisch, M., Wipf, A., Denneler, B., Battaglia, J., & Benz, C. (2000). Die Gletscher der Schweizer Alpen: Gletscherstand 1850. Aktuelle Vergletscherung, Gletscherschwundszenarien, End report NFP 31, Second Edition, Zurich, vdf Hochschulverlag, ETH Zurich, p. 373.

Meier, M. F., & Tangborn, W. V. (1961). Distinctive characteristics of glacier runoff. *US Geol. Surv. Prof. Pap*, *424*, B14–B16.

MeteoSwiss: Daily mean, minimum and maximum temperature: TabsD, TminD, TmaxD, Tech. rep., Federal Office of Meteorology and Climatology (MeteoSwiss), 2013.

MeteoSwiss: Daily Precipitation: RhiresD, Tech. rep., Federal Office of Meteorology and Climatology (MeteoSwiss), 2016.

Meyer, J., Kohn, I., Stahl, K., Hakala, K., Seibert, J., & Cannon, A. J. (2019). Effects of univariate and multivariate bias correction on hydrological impact projections in Alpine catchments. *Hydrology and Earth System Sciences*, *23*, 1339–1354. https://doi.org/10.5194/hess-23-1339-2019

Milly, P. C. D., & Wetherald, R. T. (2002). Macroscale water fluxes 3. Effects of land processes on variability of monthly river discharge. *Water Resources Research*, *38*(11), 17-1–17-12. https://doi.org/10.1029/2001wr000761

Moore, R. D. (1992). The influence of glacial cover on the variability of annual runoff, Coast Mountains, British Columbia, Canada. *Canadian Water Resources Journal*, *17*(2), 101–109. https://doi.org/10.4296/cwrj1702101

Müller, F., Catfish, T., & Müller, G. (1977). Firn und Eis der Schweizer Alpen.

Nolin, A. W., Phillippe, J., Jefferson, A., & Lewis, S. L. (2010). Present-day and future contributions of glacier runoff to summertime flows in a Pacific Northwest watershed: Implications for water resources. *Water Resources Research*, *46*(12). https://doi.org/10.1029/2009wr008968

Paul, F., Frey, H., & Le Bris, R. (2011). A new glacier inventory for the European Alps from Landsat TM scenes of 2003: Challenges and results. *Annals of Glaciology*, *52*(59), 144–152. https://doi.org/10.3189/172756411799096295

Paul, F., Kääb, A., & Haeberli, W. (2007). Recent glacier changes in the Alps observed by satellite: Consequences for future monitoring strategies. *Global and Planetary Change*, *56*(1-2), 111–122. https://doi.org/10.1016/j.gloplacha.2006.07.007

Pritchard, H. D. (2019). Asia's shrinking glaciers protect large populations from drought stress. *Nature*, *569*(7758), 649–654. https://doi.org/10.1038/s41586-019-1240-1

Rees, H. G., & Collins, D. N. (2006). Regional differences in response of flow in glacier-fed Himalayan rivers to climatic warming. *Hydrological Processes*, *20*(10), 2157–2169. https://doi.org/10.1002/hyp.6209

Rothlisberger, H., & Lang, H. (1987). Glacial hydrology. In *Glacio-fluvial sediment transfer: An Alpine perspective, Wiley-Interscience* (pp. 207–284). Chichester, United Kingdom: John Wiley and Sons. Ltd.

Schaefli, B., Manso, P., Fischer, M., Huss, M., & Farinotti, D. (2019). The role of glacier retreat for Swiss hydropower production. *Renewable Energy*, *132*, 615–627. https://doi.org/10.1016/j.renene.2018.07.104

Seibert, J., Vis, M. J., Kohn, I., Weiler, M., & Stahl, K. (2018). Representing glacier geometry changes in a semi-distributed hydrological model. *Hydrology and Earth System Sciences*, *22*(4), 2211–2224. https://doi.org/10.5194/hess-22-2211-2018

Seibert, J., & Vis, M. J. P. (2012). Teaching hydrological modeling with a user-friendly catchment runoff model software package. *Hydrology and Earth System Sciences*, *16*(9), 3315–3325. https://doi.org/10.5194/hess-163315-2012

Singh, R., Wagener, T., Werkhoven, K. V., Mann, M. E., & Crane, R. (2011). A trading-space-for-time approach to probabilistic continuous streamflow predictions in a changing climate—Accounting for changing watershed behavior. *Hydrology and Earth System Sciences*, *15*(11), 3591–3603. https://doi.org/10.5194/hess-15-3591-2011

Sivapalan, M., Yaeger, M. A., Harman, C. J., Xu, X., & Troch, P. A. (2011). Functional model of water balance variability at the catchment scale: 1. *Evidence of hydrologic similarity and space-time symmetry*. *Water Resources Research*, *47*(2). https://doi.org/10.1029/2010wr009568

Stahl, K., & Moore, R. D. (2006). Influence of watershed glacier coverage on summer streamflow in British Columbia, Canada. *Water Resources Research*, *42*(6). https://doi.org/10.1029/2006wr005022

Stahl, K., Weiler, M., Freudiger, D., Kohn, I., Seibert, J., Vis, M., … & Böhm, M. (2017). The snow and glacier melt components of streamflow of the river Rhine and its tributaries considering the influence of climate change. *Final report to the International Commission for the Hydrology of the Rhine (CHR)*, available at: www.chr-khr.org/en/publications.

Vincent, C., Fischer, A., Mayer, C., Bauder, A., Galos, S. P., Funk, M., … Huss, M. (2017). Common climatic signal from glaciers in the European Alps over the last 50 years. *Geophysical Research Letters*, *44*(3), 1376–1383. https://doi.org/10.1002/2016gl072094

Viviroli, D., Archer, D. R., Buytaert, W., Fowler, H. J., Greenwood, G., Hamlet, A. F., … Lorentz, S. (2011). Climate change and mountain water resources: Overview and recommendations for research, management and policy. *Hydrology and Earth System Sciences*, *15*(2), 471–504. https://doi.org/10.5194/hess-15-471-2011

Whitfield, P. H., Wang, J. Y., & Cannon, A. J. (2003). Modelling future streamflow extremes—Floods and low flows in Georgia basin, British Columbia. *Canadian Water Resources Journal/Revue canadienne des ressources hydriques*, *28*(4), 633–656. https://doi.org/10.4296/cwrj2804633

Zappa, M., & Kan, C. (2007). Extreme heat and runoff extremes in the Swiss Alps. *Natural Hazards and Earth System Sciences*, *7*(3), 375–389. https://doi.org/10.5194/nhess-7-375-2007

Zhang, Y., Luo, Y., Sun, L., Liu, S., Chen, X., & Wang, X. (2016). Using glacier area ratio to quantify effects of melt water on runoff. *Journal of Hydrology*, *538*, 269–277. https://doi.org/10.1016/j.jhydrol.2016.04.026

SUPPORTING INFORMATION

Additional supporting information may be found online in the Supporting Information section at the end of this article.

How to cite this article: van Tiel M, Kohn I, Van Loon AF, Stahl K. The compensating effect of glaciers: Characterizing the relation between interannual streamflow variability and glacier cover. *Hydrological Processes*. 2020;34:553–568. https://doi.org/10.1002/hyp.13603

APPENDIX

TABLE A1 Multicatchment data set for empirical analyses sorted by glacier cover. *g* is based on 2010/2012, climate data is based on 1961-2016

Catchments	Country	River	Catchment area (km^2)	Glacier area (km^2)	Glacier Cover (%)	Mean elevation (m a.s.l.)	Elevation range (m)	Mean annual P [mm/year]	Mean annual T (°C)	Streamflow data
Glacierized										
Vernagt[a,c]	AT	Vernagtbach	11.5	8.4	73.5	3122	973	1125	−4.9	1974–2015
Blatten bei Naters[c,d]	CH	Massa	195.5	110.6	56.6	2937	2741	2374.4	−3.1	1922–2016
Gletsch[c]	CH	Rhone	39.4	16.5	41.8	2709	1860	2036.5	−2.6	1956–2016
Hinterbichl UW	AT	Isel	35	13.65	39	2591	1955	1483.2	−2.4	1951–2015
Vent[c]	AT	Rofenache	98.1	32	32.7	2890	1873	976.6	−3.4	1967–2015
Ochsenhütte	AT	Hochalmbach	8.73	2.6	29.9	2663	1356	1562.9	−2	1961–2015
Innergschlöss	AT	Gschlössbach	40	11.3	28.4	2463	2139	1723.5	−1.7	1951–2015
Obergurgl	AT	Gurgler Ache	73	19	26	2782	1629	984.8	−2.6	1966–2015
Blatten[c,d]	CH	Lonza	77.4	19.1	24.7	2620	2376	1758.7	−2.1	1956–2016
Oberried/Lenk[c,d]	CH	Simme	34.8	7.8	22.5	2341	2147	1892.7	−1.1	1944–2016
Erstfeld-Bodenberg[c]	CH	Alpbach	20.7	4.1	19.6	2193	2170	1619.3	0.6	1960–2016
Matreier Tauernhaus	AT	Tauernbach	60.28	11.33	18.8	2463	2139	1675.1	−0.9	1951–2015
Sulzau	AT	Obersulzbach	80.8	14.3	17.7	2298	2772	1603.8	0.1	1961–2015
Huben	AT	Öztaler Ache	516.9	80.7	15.6	2621	2577	972.6	−1.7	1976–2015
Pontresina[b,c,d]	CH	Berninabach	106.9	15.3	14.4	2614	2214	1242.4	−2.2	1954–2016
Gsteig[d]	CH	Lütschine	380.7	51.4	13.5	2040	2308	1809.3	0.6	1908–2016
Zweilütschinen[c]	CH	Weisse Lütschine	164.9	21.5	13.1	2150	3495	1848.6	0.3	1933–2016
Spöttling-taurer	AT	Teilschnitzbach	14	1.8	13.1	2295	2722	1263.8	−1.7	1976–2015
Neukirchen	AT	Untersulzbach	40.5	4.9	12.1	2167	2441	1496.1	0.9	1971–2015
Spöttling	AT	Kalserbach	47	4.9	10.3	2594	2295	1540	−0.9	1951–2015
Neukaser	AT	Zamserbach	24.4	2.1	8.6	2506	1676	1387.6	−1.2	1976–2015
Hinterbichl	AT	Islitz	107	8.95	8.4	2538	2164	1395.6	−1.5	1951–2015
Waier	AT	Isel	285.3	22.9	8	2660	2308	1279.4	−0.1	1951–2015
Isenthal[c]	CH	Grosstalbach	43.9	2.9	6.7	1814	2170	1768.1	2.5	1956–2016
Buochs[b,d]	CH	Engelberger Aa	228	5.6	2.5	1604	2784	1813.4	2.9	1916–2016
Oberwil	CH	Simme	343.7	8.2	2.4	1635	2466	1790.5	0.6	1921–2016
Sumvitg-Encardens[c,d]	CH	Rein da Sumvitg	21.8	0.4	1.7	2447	1670	1656.1	−0.9	1932–2016

(Continues)

TABLE A1 (Continued)

Catchments	Country	River	Catchment area (km^2)	Glacier area (km^2)	Glacier Cover (%)	Mean elevation (m a.s.l.)	Elevation range (m)	Mean annual P [mm/year]	Mean annual T (°C)	Streamflow data
St. Jodok	AT	Schmirnbach	108.8	0.9	0.8	2020	2349	1172.2	1.7	1951–2015
Davos[c]	CH	Dischmabach	42.9	0.3	0.65	2372	1474	995.9	−0.7	1963–2016
Hopfgarten	AT	Schwarzbach	268.6	1.7	0.6	2451	2066	1175	0.1	1951–2015
Mallnitz	AT	Mallnitzbach	85.3	0.4	0.5	2040	2183	1289	1.5	1961–2015
Puig	AT	Sill	341.8	1.2	0.4	1910	2465	1187.9	2.3	1951–2015
Steinach	AT	Gschnitzbach	111.4	0.3	0.3	1952	2190	1263.7	2.1	1951–2015
La Punt-Chamues-ch[c]	CH	Chamuerabach	73.4	0.05	0.07	2547	1536	1084.9	−2.1	1954–2016
Zernez	CH	Ova da Cluozza	27	0	0	2366	1641	940.6	−1.2	1961–2016
Non-glacierized										
Emmenmatt	CH	Emme	443.02	0	0	1064.8	1579	1600	6.2	1974–2015
Sensematt	CH	Sense	351.17	0	0	1071.9	1626.3	1446	6.3	1961–2015
Adelboden	CH	Allenbach	28.79	0	0	1863.2	1434.5	1654	2.9	1961–2015
Eggiwil	CH	Emme	124.36	0	0	1281.2	1607.6	1676	5.1	1975–2015

Note. g is based on 2010/2012; climate data is based on 1961–2016.

[a]Infilled winter streamflow data.

[b]Possibly influenced (e.g., hydropeaking).

[c]Overlapping catchment with CO1990 study.

[d]Catchment with long time series used for CV_Q changes over time (Figure 7).